DOI: https://doi.org/10.33103/uot.ijccce.22.4.7

Fractional Order Fuzzy Like PID Controller Design for Three Links Rigid Robot Manipulator

Hadeel I. Abdulameer[1], Mohamed J. Mohamed[2]
[1,2]Control and Systems Engineering Department, University of Technology, Baghdad, Iraq
[1]cse.19.13@grad.uotechnology.edu.iq, [2]Mohamed.J.Mohamed@uotechnology.edu.iq

Abstract— *Four Fractional/Integer Order Fuzzy Proportional Integral Derivative controller structures are designed in this study to successfully control a nonlinear, coupled, multi-input, multi-output, three-link rigid robotic manipulator system. The performance of Fractional Order Fuzzy Proportional Integral Derivative and Integer Order Fuzzy Proportional Integral Derivative controllers is evaluated for reference trajectory tracking, changing beginning circumstances, disturbance rejection, and model uncertainty. These controllers' parameters are tuned using a meta-heuristic optimization approach called the most valuable player algorithm for the objective function, which is defined as the integral of the time-squared error. Simulation results show that the suggested Fractional Order Fuzzy Proportional Integral Derivative controllers outperform Integer Order Fuzzy Proportional Integral Derivative controllers for tracking performance, stability, and robustness for all structures. Fractional Order Fuzzy Proportional Derivative Fractional Order Proportional Integral Derivative controller is the best one for trajectory tracking, disturbances rejection, and parameter variation with the least integral of time square error equal to 2.7420×10^{-6}, 3.4×10^{-3} and 2.0108×10^{-4} respectively and the response of the angular position for all links for trajectory tracking has minimum settling time which is equal to 0.0290 s for the first link, 0.0160 s for the second link and 0.0050 s for the third link. When the initial condition is changed, the One Block Fractional Order Fuzzy Proportional Integral Derivative controller is the best one, since the integral of time square error is minimum and equal to 1.6253×10^{-4}.*

Index Terms— *Fractional order controller, Fuzzy logic, Most valuable player algorithm, PID controller, Robotic manipulator.*

I. INTRODUCTION

In recent years, robot manipulators have become increasingly common in industrial applications. Industrial robot manipulators are essentially positioning and handling devices. A very wide range of applications was found, which include cargo loading and unloading, automatic assembly lines, spray paint application, handling dangerous radioactive materials, forging and military use. As a result, an effective robot manipulator can control its motion as well as the forces it produces on its surroundings. In fact, industrial robot manipulators are multi-input, multi-output nonlinear systems that are sensitive to external disturbances, nonlinear friction, and payload variation. So it is difficult to design an accurate controller without understanding the robot system [1],[2].

Designing a simple controller with asymptotic tracking performance for robot manipulator systems has become a fundamental criterion for researchers and engineers. Many researchers are interested in using fuzzy controllers since in comparison to other

Received 09/February/2022; Accepted 30/April/2022
 ISSN (Print) 1811-9212 ISSN (Online) 2617-3352

DOI: https://doi.org/10.33103/uot.ijccce.22.4.7

nonlinear controllers, they are superior due to their robustness, simplicity, efficiency, and universal approximation property [3].

When fractional-order mathematical operators are merged with a fuzzy logic controller, the degree of freedom is increased and an accurate solution is achieved which has been used in the field of control in a variety of applications [4]. Furthermore, to fit the controlled system specifications, the controller's robustness can be improved by combining fractional-order actions with more strong and flexible design techniques [5].

In the past few years, 3-Link Rigid Robot Manipulator (3-LRRM) system has been intensively studied by many researchers. In [6], the dynamics of the 3-LRRM combined with a camera for capturing the user's motion system were derived and the angles of each link were controlled by using a PD controller. The simulation results demonstrated the effectiveness of a PD controller. The main problems with this study were that the robust concept was not achieved and the controller's parameters were not optimized by any optimization method. A robust Fractional Order Fuzzy Proportional Derivative plus Fractional Order Integrator (FOFPD+FOI) control structure was presented in [4] to effectively control a nonlinear electrically driven 3-LRRM system. A comparison of the performance of the FOFPD+FOI controller with the IOFPD+IOI controller, the fractional-order proportional, integral, and derivative (FOPID) controller, and the integer-order PID controller was performed for reference trajectory tracking, noise suppression, disturbance rejection, and model uncertainty. Simulation results showed that the proposed FOFPD+FOI controller outperforms PID, FOPID and IOFPD+IOI controllers significantly.

Three different position control methodologies were designed and analyzed for a 3-DOF robot manipulator in [7]. Each link of the robot manipulator was controlled with PID, PD and FLC controllers. The PID and PD controllers outperformed the FLC in terms of rising time and settling time whereas the FLC had less overshoot. The main problems with this study were that the robust concept was not achieved and the controller's parameters were not optimized by any optimization method.

A Self-Regulated Fractional-Order Fuzzy Proportional–Integral–Derivative (SRFOFPID) controller was presented and successfully tested in simulation to effectively control a 3-LRRM in [8]. The results of the study illustrated that fractional operators increase the degree of freedom and robustness of the SRFOFPID controller. A fuzzy logic controller for a 3-DOF robot manipulator was presented in [9]. The simulation results demonstrated that PID produces better transient parameters. In steady state response, both the PID and the FLC converge to their desired performance but the overwhelming FLC exceeds null. The main problems with this study were that the robust concept was not achieved.

A fuzzy fractional order (FO) adaptive impedance controller was presented on the robot manipulator to prevent force overshoots in the contact stage while keeping force error in the dynamic tracking stage where conventional control methods are ineffective[10]. The simulation results showed that the suggested controller can be designed to be more stable and superior to the general impedance controller and the force tracking results have also been compared to earlier control methods.

In this work, we will use four structures of the Fractional/Integer Order Fuzzy PID controller (FOFPID, IOFPID). The gains of all structures of the controller are tuned using the Most Valuable Player Algorithm (MVPA) to minimize the Integral of the Time Squared Error (ITSE). A comparison has been made for all controllers for trajectory tracking performance, changing initial conditions, disturbance rejection, and model uncertainties.

Received 09/February/2022; Accepted 30/April/2022
 ISSN (Print) 1811-9212 ISSN (Online) 2617-3352

DOI: https://doi.org/10.33103/uot.ijccce.22.4.7

The rest of this paper is organized as follows: Section II describes the dynamic model of the 3-LRRM. In section III, the proposed FOFPID and IOFPID controllers are illustrated. MVPA is displayed in section IV. Section V presents the simulation results. Finally, the conclusion is given in section VI.

II. THE DYNAMIC MODEL OF 3-LRRM

A robotic manipulator is made up of a sequence of links, each link is connected to its neighboring link with a joint. The movement of a planar robotic manipulator is limited to one plane only. Planar robotic manipulators are used as prototypes in a variety of industrial robotic systems for assisted automation and medical applications. As a result, researchers have been interested in the problem of controlling the position and orientation of a planar robotic manipulator [11]. In this work, a planar robotic manipulator with three revolute joints is considered and all of its joints are assumed to be actuated.

A three-link planar rigid robotic manipulator system with three degrees of freedom is depicted in *Fig. 1*. A frictionless pivot connects the system's first link to a rigid bottom and a frictionless ball bearing connects the second link to the end of the first link also frictionless ball bearings connect the third and second links [12]. In robotics, the dynamic equation of motion of the manipulator is used to build up the basic control equations. The torques provided by the actuators are used to generate the manipulator's arm dynamic motion in a robotic system[13]. The dynamic model of a three-link planar rigid robotic manipulator is as follows.

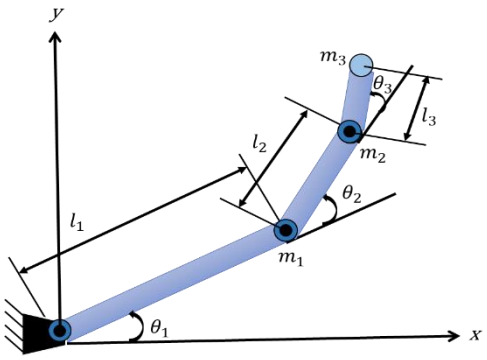

FIG. 1. THE STRUCTURE OF 3-LRRM[12].

The equations for the *x* and *y* positions of mass of link1 m_1 are given by:

$$x_1 = l_1 \cos(\theta_1) \quad (1)$$

$$y_1 = l_1 \sin(\theta_1) \quad (2)$$

Similarly, the equations for the *x* and *y* positions of mass of link2 m_2 are given by:

$$x_2 = l_1 \cos(\theta_1) + l_2 \cos(\theta_1 + \theta_2) \quad (3)$$

$$y_2 = l_1 \sin(\theta_1) + l_2 \sin(\theta_1 + \theta_2) \quad (4)$$

While the *x* and *y* positions of mass of link3 m_3 are given by:

$$x_3 = l_1 \cos(\theta_1) + l_2 \cos(\theta_1 + \theta_2) + l_3 \cos(\theta_1 + \theta_2 + \theta_3) \quad (5)$$

$$y_3 = l_1 \sin(\theta_1) + l_2 \sin(\theta_1 + \theta_2) + l_3 \sin(\theta_1 + \theta_2 + \theta_3) \quad (6)$$

The kinetic energy *KE* is defined as:

$$KE = \frac{1}{2} m_1 v_1^2 + \frac{1}{2} m_2 v_2^2 + \frac{1}{2} m_3 v_3^2 \quad (7)$$

Where V_1, V_2 and V_3 are the velocities for m_1 , m_2 , and m_3 respectively and can be calculated as:

$$V_1 = \sqrt{\dot{x}_1^2 + \dot{y}_1^2} \quad , \quad V_2 = \sqrt{\dot{x}_2^2 + \dot{y}_2^2} \quad , \quad V_3 = \sqrt{\dot{x}_3^2 + \dot{y}_3^2} \quad (8)$$

Received 09/February/2022; Accepted 30/April/2022

ISSN (Print) 1811-9212 ISSN (Online) 2617-3352

DOI: https://doi.org/10.33103/uot.ijccce.22.4.7

So the kinetic energy will be:

$$KE = \frac{1}{2}m_1(\dot{x}_1^2 + \dot{y}_1^2) + \frac{1}{2}m_2(\dot{x}_2^2 + \dot{y}_2^2) + \frac{1}{2}m_3(\dot{x}_3^2 + \dot{y}_3^2) \quad (9)$$

And the potential energy *PE* can be written as:

$$PE = \sum_{i=1}^{3} m_i\ g\ h_i(\theta) \quad (10)$$

Where *h* is the height of the mass center for each link. Hence *PE* can be written as:

$$PE = m_1\ g\ l_1\ sin(\theta_1) + m_2\ g(l_1\ sin(\theta_1) + l_2\ sin(\theta_1 + \theta_2)) + m_3\ g(\ l_1\ sin(\theta_1) + \ l_2\ sin(\theta_1 + \theta_2) + l_3\ sin(\theta_1 + \theta_2 + \theta_3) \quad (11)$$

Next, by using the Lagrange Dynamic, we form the Lagrangian which is defined as:

$$L = KE - PE \quad (12)$$

The Euler-Lagrange Equation is given by:

$$\frac{d}{dt}\left[\frac{\partial L}{\partial \dot{\theta}_i}\right] - \frac{\partial L}{\partial \theta_i} = F\theta_i \quad (13)$$

Where $F\theta_i$ is the torque applied to the i^{th} link.

These manipulator dynamics are in the standard form [14].

$$D(\theta)\ddot{\theta} + P(\theta, \dot{\theta}^2) + R(\theta, \dot{\theta}_i\dot{\theta}_j) + G(\theta) = \tau \quad (14)$$

Where $D(\theta)$ is the inertia matrix

$$D = \begin{bmatrix} D_{11} & D_{12} & D_{13} \\ D_{21} & D_{22} & D_{23} \\ D_{31} & D_{32} & D_{33} \end{bmatrix}$$

$$D_{11} = (m_1 + m_2 + m_3)l_1^2 + (m_2 + m_3)l_2^2 + m_3l_3^2 + 2m_3l_1l_3\ cos(\theta_2 + \theta_3] + 2(m_2 + m_3)l_1l_2\ cos(\theta_2) + 2m_3l_2l_3cos(\theta_3)$$

$$D_{12} = (m_2 + m_3)l_2^2 + m_3l_3^2 + m_3l_1l_3\ cos(\theta_2 + \theta_3) + (m_2 + m_3)l_1l_2\ cos(\theta_2) + 2m_3l_2l_3cos(\theta_3)$$

$$D_{13} = m_3l_3^2 + m_3l_1l_3\ cos(\theta_2 + \theta_3) + m_3l_2l_3cos(\theta_3)$$

$$D_{21} = m_2l_2^2 + m_3l_2^2 + m_3l_3^2 + m_3l_1l_3\ cos(\theta_2 + \theta_3) + m_2l_1l_2\ cos(\theta_2) + m_3l_1l_2\ cos(\theta_2) + 2m_3l_2l_3cos(\theta_3)$$

$$D_{22} = m_2l_2^2 + m_3l_2^2 + m_3l_3^2 + 2m_3l_2l_3cos(\theta_3)$$

$$D_{23} = m_3l_3^2 + m_3l_2l_3cos(\theta_3)$$

$$D_{31} = m_3l_3^2 + m_3l_1l_3\ cos(\theta_2 + \theta_3) + m_3l_2l_3cos(\theta_3)$$

$$D_{32} = m_3l_3^2 + m_3l_2l_3cos(\theta_3)$$

$$D_{33} = m_3l_3^2$$

$P = \begin{bmatrix} P_1 \\ P_2 \\ P_3 \end{bmatrix}$ are the Centrifugal terms which are defined as;

$$P_1 = -l_1(m_3l_3\ sin(\theta_2 + \theta_3) + m_2l_2\ sin(\theta_2) + m_3l_2\ sin(\theta_2))\ \dot{\theta}_2^2 - m_3l_3(l_1\ sin(\theta_2 + \theta_3) + l_2\ sin(\theta_3))\dot{\theta}_3^2$$

$$P_2 = l_1(m_3l_3\ sin(\theta_2 + \theta_3) + m_2l_2\ sin(\theta_2) + m_3l_2\ sin(\theta_2))\dot{\theta}_1^2 - m_3l_2l_3sin(\theta_3)\dot{\theta}_3^2$$

$$P_3 = m_3l_3(l_1\ sin(\theta_2 + \theta_3) + l_2\ sin(\theta_3))\dot{\theta}_1^2 + m_3l_2l_3sin(\theta_3)\dot{\theta}_2^2$$

$R = \begin{bmatrix} R_1 \\ R_2 \\ R_3 \end{bmatrix}$ are the Coriolis terms which are defined as;

$$R_1 = -2l_1(m_3l_3\ sin(\theta_2 + \theta_3) + (m_2 + m_3)l_2\ sin(\theta_2))\dot{\theta}_1\dot{\theta}_2 - 2m_3l_3(l_1\ sin(\theta_2 + \theta_3) + l_2\ sin(\theta_3))\dot{\theta}_2\dot{\theta}_3 - 2m_3l_3(l_1\ sin(\theta_2 + \theta_3) + l_2\ sin(\theta_3))\dot{\theta}_1\dot{\theta}_3$$

$$R_2 = -2m_3l_2l_3\ sin(\theta_3)\ \dot{\theta}_1\dot{\theta}_3 - 2m_3l_2l_3sin(\theta_3)\dot{\theta}_2\dot{\theta}_3$$

$$R_3 = 2m_3l_2l_3sin(\theta_3)\dot{\theta}_1\dot{\theta}_2$$

Received 09/February/2022; Accepted 30/April/2022

ISSN (Print) 1811-9212 ISSN (Online) 2617-3352

DOI: https://doi.org/10.33103/uot.ijccce.22.4.7

$G = \begin{bmatrix} G_1 \\ G_2 \\ G_3 \end{bmatrix}$ are the Potential energy terms which are defined as;

$G_1 = (m_1 + m_2 + m_3) g l_1 \cos(\theta_1) + (m_2 + m_3) g l_2 \cos(\theta_1 + \theta_2) + m_3 g l_3 \cos(\theta_1 + \theta_2 + \theta_3)$

$G_2 = (m_2 + m_3) g l_2 \cos(\theta_1 + \theta_2) + m_3 g l_3 \cos(\theta_1 + \theta_2 + \theta_3)$

$G_3 = m_3 g l_3 \cos(\theta_1 + \theta_2 + \theta_3)$

The coordinates of the end-effector of the 3-LRRM can be obtained from joint angles θ_{r1}, θ_{r2} & θ_{r3} using forward kinematic [15] as it is given in the following equations:

$$x_r = l_1 \cos(\theta_{r1}) + l_2 \cos(\theta_{r1} + \theta_{r2}) + l_3 \cos(\theta_{r1} + \theta_{r2} + \theta_{r3}) \quad (15)$$

$$y_r = l_1 \sin(\theta_{r1}) + l_2 \sin(\theta_{r1} + \theta_{r2}) + l_3 \sin(\theta_{r1} + \theta_{r2} + \theta_{r3}) \quad (16)$$

Where θ_{r1},θ_{r2}, and θ_{r3} are the desired trajectories.

The parameters that are considered in this work is given in Table I.

TABLE I. THE PARAMETERS OF 3-LRRM[12]

parameters	Nominal value
m_1	0.1 kg
m_2	0.1 kg
m_3	0.1 kg
l_1	0.8 m
l_2	0.4 m
l_3	0.2 m
g	9.81 m/s^2

The feedback linearization is used to compute the required arm torques using the nonlinear feedback control law and it is used for decoupling among links[16].

III. CONTROLLER DESIGN

In this section, we will give an overview of the proposed controller's components for the 3-LRRM and describe the nature and structures of these controllers.

A. The Proposed Controllers' Components

In the following, we will explain the main components of the proposed controllers to illustrate the process of completing the design of these controllers.

i. PID Controller

One of the most widely used control techniques is the PID controller. It is simple in implementation so it is applied to a wide range of applications. The PID controller can be represented as:

$$u(t) = K_p \left(e(t) + \frac{1}{T_i} \int e(t)\, dt + T_d\, \dot{e}(t) \right) \quad (17)$$

Where $u(t)$ represents the control action, $e(t)$ represents the error and $\dot{e}(t)$ represents the change of error, and K_p represents the proportional gain and provides a control action proportional to the error signal $e(t)$, T_d is the derivative term that produces a control signal

Received 09/February/2022; Accepted 30/April/2022
 ISSN (Print) 1811-9212 ISSN (Online) 2617-3352

DOI: https://doi.org/10.33103/uot.ijccce.22.4.7

proportional to the change of error with respect to time, resulting in output overshoot damping and thus improved transient response and T_i is the integral term that decreases the steady-state error by continuous integration of the error signal $e(t)$ [17].

ii. Fractional Order PID Controller

Podlubny introduced the FOPID controller in 1999[18]. The FOPID controller is an extension of the conventional PID controller that enables the integration and differentiation actions to be performed in any order. The differential equation of the $PI^{\lambda}D^{\mu}$ controller in the time domain is expressed as:

$$u(t) = K_p\, e(t) + K_i D^{-\lambda}\, e(t) + K_d\, D^{\mu}\, e(t) \tag{18}$$

If $\lambda = \mu = 1$, a conventional integer-order PID controller is generated, if λ=0, and μ=1, a conventional integer- order PD controller is generated, and if λ=1, and μ=0, a conventional integer-order PI controller is generated. *Fig. 2* depicts the plane of the PID controller's integral and derivative actions with extra freedom in adjusting the orders of the FOPID controller. The typical PID controller can clearly be defined by only four points in the plane but the FOPID controller can be described by the whole restricted plane [18].

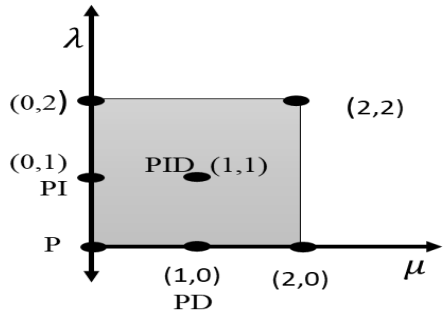

FIG. 2. THE ORDER OF DERIVATIVE AND INTEGRAL OF PID AND FOPID[18].

There are numerous ways to describe non-integer integration and differentiation. The most commonly used definitions are those of Grünwald–Letnikov (GL), Riemann–Liouville (RL), and Caputo [19]. The GL definition is:

$${}_aD_t^{\alpha}\, f(t) = \lim_{h\to 0} \frac{1}{h^{\alpha}} \sum_{j=0}^{\left[\frac{t-a}{h}\right]} (-1)^j \binom{\alpha}{j} f(t-jh) \tag{19}$$

While the RL definition is given by:

$${}_aD_t^{\alpha}\, f(t) = \frac{1}{\Gamma(n-\alpha)} \frac{d^n}{dt^n} \int_a^t \frac{f(\tau)}{(t-\tau)^{\alpha-n+1}} \tag{20}$$

For (n-1<α<n) and $\Gamma(x)$ is the well-known Euler's Gamma function.

$$g\,(t, x, {}_aD_t^{\alpha 1} x, {}_aD_t^{\alpha 2} x \ldots) = 0 \qquad \text{Where } \alpha_k \in R^{+}. \tag{21}$$

Caputo's definition can be written as

$${}_aD_t^{\alpha}\, f(t) = \frac{1}{\Gamma(\alpha-n)} \int_a^t \frac{f^{(n)}}{(t-\tau)^{\alpha-n+1}}\, d\tau \qquad \text{For } (n-1 < \alpha < n) \tag{22}$$

iii. Fuzzy Logic Controller (FLC)

To introduce human decision-making and experience to the plant, Fuzzy Logic Controllers (FLCs) are represented to the system to include the intelligence to the controller. The relationships between the input and output are represented using a set of linguistic rules or relational expressions[20]. Fuzzy systems have been employed in a variety of areas including engineering, technology, business, medical, psychology, and others. The fuzzy controller is made up of four

Received 09/February/2022; Accepted 30/April/2022
 ISSN (Print) 1811-9212 ISSN (Online) 2617-3352

DOI: https://doi.org/10.33103/uot.ijccce.22.4.7

fundamental components: the first one is the rule-base which contains a set of rules for the most effective control of the system that represents the knowledge. The second part is the inference mechanism which decides which control rules are applicable at the current circumstance and then determines what should be the output of the controller to the plant. The third part is the fuzzification interface which simply modifies the inputs so that they can match the rules of the rule base. The final part is the defuzzification interface that transforms the inference mechanism's conclusions into the inputs to the plant [21],[22]. These elements are shown in *Fig*. 3.

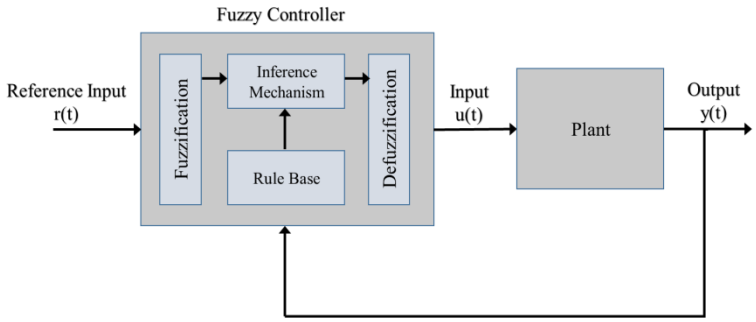

FIG. 3. THE STRUCTURE OF THE FUZZY CONTROLLER[23].

B. The Structures of The Proposed Controller

Four structures of FOFPID and IOFPID controllers are presented to control the trajectory tracking of the 3-LRRM.

i. Fractional/Integer Order Fuzzy PD + I Controller Structure (FOFPD+I/IOFPD+I)

The general block structure of the Fractional/Integer Order Fuzzy PD+I controller for trajectory tracking of the 3-LRRM is illustrated in *Fig. 4*, which demonstrates the separate controller for each input of 3-LRRM control where the reference trajectory is compared to the actual trajectory for each link. The input variables for the fuzzy controller are the error e and its change $\dot{e}$.

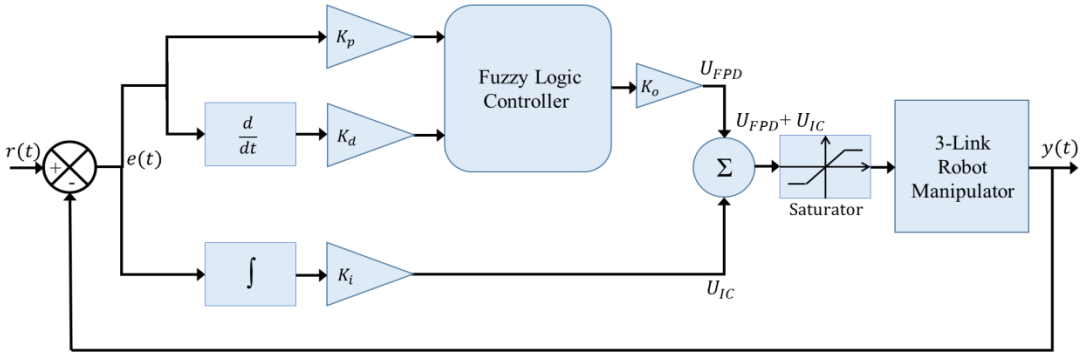

FIG. 4. THE STRUCTURE OF THE FRACTIONAL/INTEGER ORDER FUZZY PD+I CONTROLLER FOR 3-LRRM[24].

There is only one fuzzy proportional-differential control block in the fuzzy controller and no fuzzy integral control block. The Integral Control (IC) is used in conjunction with the fuzzy PD controller to improve the performance of the steady-state of the system [24].

ii. One Block Fractional/Integer Order Fuzzy PID Controller Structure (OBFOFPID/OBIOFPID)

The distinct controller for each input of 3-LRRM controlling of the One Block Fractional/Integer Order Fuzzy PID controller is shown in *Fig. 5*. This controller is constructed as a summation of the fuzzy PD controller and the fuzzy PI controller when the output of the fuzzy PD is given to the

Received 09/February/2022; Accepted 30/April/2022

ISSN (Print) 1811-9212 ISSN (Online) 2617-3352

DOI: https://doi.org/10.33103/uot.ijccce.22.4.7

integrator to produce a fuzzy PI controller. The input variables for the fuzzy controller are error e and derivative of the error $\dot{e}$ and the output is control signal u [25].

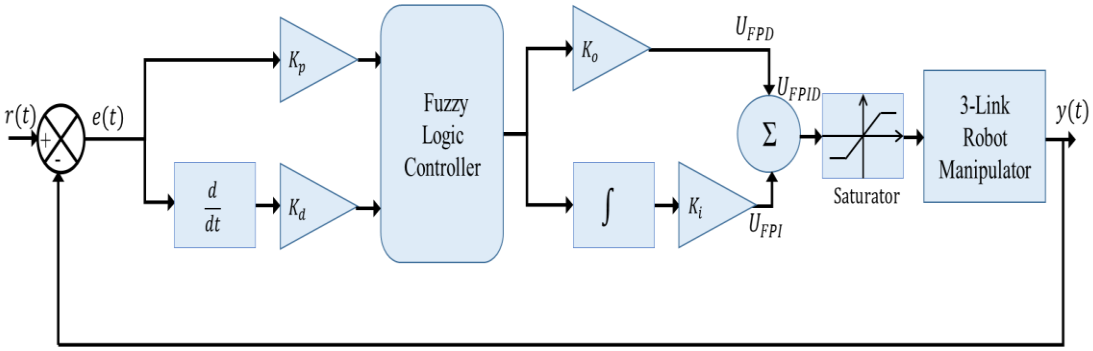

FIG. 5. THE STRUCTURE OF THE ONE BLOCK FRACTIONAL/INTEGER ORDER FUZZY PID CONTROLLER FOR 3-LRRM[25].

iii. Two-Block Fractional/Integer Order Fuzzy PID Controller Structure (TBFOFPID/TBIOFPID)

The general structure of the Two-Block Fractional/Integer Order Fuzzy PID controller is shown in *Fig. 6* which represents the individual controller for each input of 3-LRRM control. Fuzzy PI control is known to be more practical than fuzzy PD because it is difficult for fuzzy PD to eliminate steady-state error. However, because of the internal integration operation, the fuzzy PI control is known to perform poorly in transient response for higher-order systems. It is easy and convenient to combine PI and PD actions to construct a fuzzy PID-type controller to provide proportional, integral and derivative control actions together at once. As a result, by combining fuzzy PI and PD controllers with two distinct rule-bases, a fuzzy PID controller can be constructed [26],[27].

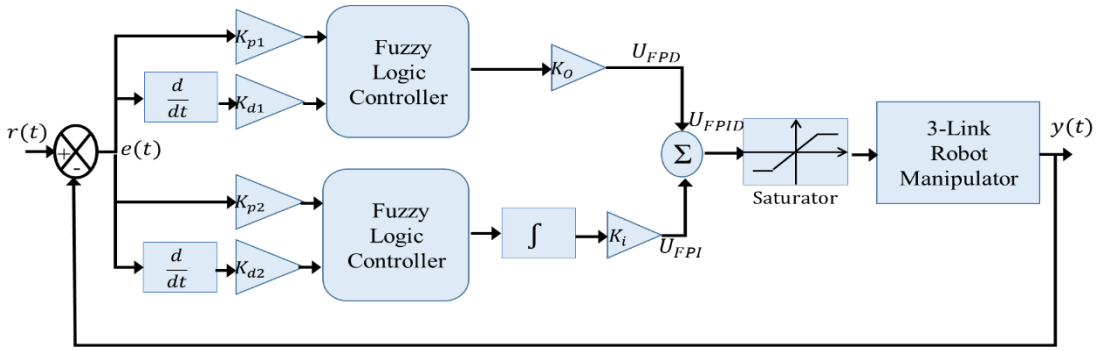

FIG. 6. THE STRUCTURE OF THE TWO-BLOCK FRACTIONAL/INTEGER ORDER FUZZY PID CONTROLLER FOR 3-LRRM[26].

iv. Fractional/Integer Order Fuzzy PD- Fractional/Integer Order PID Controller Structure (FOFPD-FOPID/IOFPD-IOPID)

The separate controller for each input of 3-LRRM controlling of the Fractional/Integer Order Fuzzy PD- Fractional/Integer Order PID controller is illustrated in *Fig.*7.

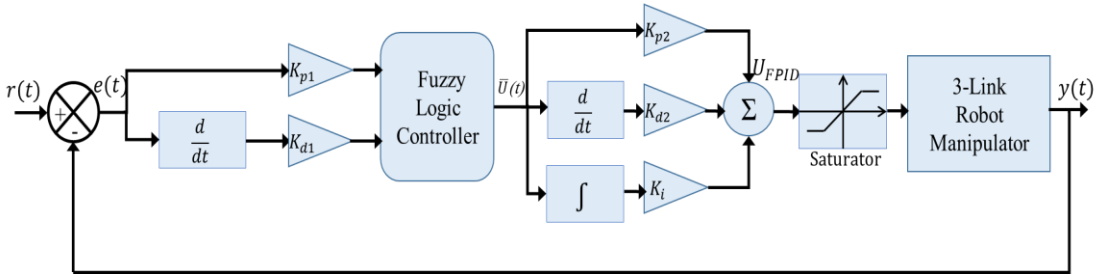

FIG. 7. THE STRUCTURE OF THE FRACTIONAL/INTEGER ORDER FUZZY PD- FRACTIONAL/INTEGER ORDER PID CONTROLLER FOR 3-LRRM[28].

Received 09/February/2022; Accepted 30/April/2022

ISSN (Print) 1811-9212 ISSN (Online) 2617-3352

DOI: https://doi.org/10.33103/uot.ijccce.22.4.7

This controller is composed of a fuzzy PD and a PID controller in which the output of the fuzzy PD will be fed to the PID controller where the fuzzy controller uses error e and the derivative of the error $\dot{e}$ as input signals [28].

In this study, seven Gaussian membership functions (MF) as "Negative large (NL)", "Negative Medium (NM)", "Negative Small (NS)", "Zero (Z)", "Positive Small (PS)", "Positive Medium (PM)" and at last, "Positive Large (PL)" are selected for each input signal and control signal U, the universe of discourse chosen to be [-10 10], Center of Gravity (COG) or (Centroid) method is used for Defuzzification, Mamdani's fuzzy inference method are employed where the rules in the rule base are as shown in Table II.

TABLE II. RULE BASE FOR AN ERROR, DERIVATIVE ERROR, AND FLC OUTPUT

$\dot{e}$ \ e	**NL**	**NM**	**NS**	**Z**	**PS**	**PM**	**PL**
NL	NL	NL	NL	NL	NM	NS	Z
NM	NL	NL	NL	NM	NS	Z	PS
NS	NL	NL	NM	NS	Z	PS	PM
Z	NL	NM	NS	Z	PS	PM	PL
PS	NM	NS	Z	PS	PM	PL	PL
PM	NS	Z	PS	PM	PL	PL	PL
PL	Z	PS	PM	PL	PL	PL	PL

IV. MOST VALUABLE PLAYER ALGORITHM

MVPA is a newly created algorithm that introduced in 2017. The MVPA is a population-based method depends on a sporting notion. In this strategy, players create teams and these teams compete to win the championship. Furthermore, each player competes in his team for the MVP trophy [29].

A. The Steps of the Most Valuable Player Algorithm

1- Initialization: a population of players is generated at random in the search space. Each player and team can be represented as follows:

$$Player_k = [S_{k,1} \;\; S_{k,2} \dots\dots S_{k,Problem\ Size}] \tag{23}$$

$$TEAM_i = \begin{bmatrix} Player_1 \\ Player_2 \\ \vdots \\ Player_{Players\ Size} \end{bmatrix} \tag{24}$$

Where *S* denotes skill, *Players Size* is the number of players in the league, and *Problem Size* is the dimension of the problem. Every team has a Franchise Player, and the league MVP is the league's best player.

2 - Teams formation: teams are formed by randomly distributing for players.

3 -Competition phase: in this phase, there are two steps:

- Individual competition

Each player aims to be the franchise player for his team as well as the MVP of the league. The skills for players are updated as follows:

$$skill_{i+1} = skill_i + rand \times (skill(Franchise\ Player_i) - skill_i) + 2 \times rand \times (skill(MVP) - skill_i) \tag{25}$$

Where *rand* is a random number distributed randomly between 0 and 1, *Franchise Player* is the best player in the team.

- Team competition: In this phase, the selected $TEAM_i$ competes against $TEAM_j$, which is chosen at random where ($i \neq j$).

The fitness of a team is the fitness of the Franchise Player of that team and it is normalized in the MVPA as follows:

$$fitnessN(TEAM_i) = fitness(TEAM_i) - min\big(fitness(All\ Teams)\big) \tag{26}$$

Received 09/February/2022; Accepted 30/April/2022
 ISSN (Print) 1811-9212 ISSN (Online) 2617-3352

DOI: https://doi.org/10.33103/uot.ijccce.22.4.7

Then, the probability that $TEAM_i$ beats $TEAM_j$ is calculated using the following formula:

$$Pr\{TEAM_i \ beats \ TEAM_j\} = 1 - \frac{(fitnessN(TEAM_i))^k}{(fitnessN(TEAM_i))^k + (fitnessN(TEAM_j))^k} \quad (27)$$

Finally, if $TEAM_i$ is chosen and plays against $TEAM_j$ in the team competition phase and if $TEAM_i$ wins, the $TEAM_i$ player skills are updated using the following expression:

$$skill_{i+1} = skill_i + rand \times \left(skill_i - skill(Franchise\ Player_j)\right) \quad (28)$$

Otherwise, the player's skills of $TEAM_i$ are updated using the following expression:

$$skill_{i+1} = skill_i + rand \times (skill(Franchise\ Player_j) - skill_i) \quad (29)$$

It should be remembered that a player's skills have lower and upper limits and all players are actively trying to improve their skills in each competition. Therefore, if a player's skills have been updated outside of these limits, the skills must be brought back to their bounds.

4- Application of greediness: after each step of competition (individual and team competition) a comparison has been done between the population before and after the competition phase, and a new solution is accepted if it produces a better result than the initial.
5- Remove duplicates: if two players in the population are equivalent, the second player is replaced by another player.
6- Use of elitism: during this phase, the worst players are replaced by the best. The number of elite players is chosen as the third of the Players Size.
7- Termination criterion: the algorithm repeats several times. The number of iterations is specified by MaxNFix (maximum number of fixtures) [29], [30].

V. SIMULATION AND RESULTS

This section discusses the performance of trajectory tracking as well as the robustness of the FOFPID and IOFPID controllers. MATLAB 2018b code is used to create the 3-LRRM, proposed controllers, and test trajectory, and the fuzzy toolbox is used to design the fuzzy controller. The simulation time is considered to be 10 s and the sampling time is assumed to be 1 ms. The torque constraints for all links were taken as [-200,200] N-m. Furthermore, the 11th order Oustaloup's approximation (N = 5) is assumed for the fraction operator design and it is in the frequency range [0.001, 1000] rad/s. A test trajectory tracking of each link is analyzed for the manipulator model to follow it and the objective function has been taken as the integral of time square error (ITSE) which is used to ensure that the error is reduced as well as speeding up the tracking of the desired path.

Depending on the tracking error between the actual path and the reference path for the 3-LRRM, the MVPA was used to tune the parameters of the FOFPID and IOFPID controllers when the initial positions are (0.1,-0.6,-0.9)rad for θ_1,θ_2 and θ_3, respectively. The MVPA setting is as follows: the population size is 40, the team size is 5, the team players are 8 and the maximum number of iterations is 100. The computation of the ITSE is used to evaluate the performance of FOFPID and IOFPID controllers. The controller that has the least ITSE is considered the best controller. The ITSE can be calculated using the following formula:

$$ITSE = \int (t \times e_1^2(t) + t \times e_2^2(t) + t \times e_3^2(t))\, dt \quad (30)$$

Where $e_1(t)$, $e_2(t)$, and $e_3(t)$ are the difference between the desired and actual trajectories for link1,link2, and link3 respectively. The desired trajectories θ_{r1},θ_{r2} and θ_{r3} have been given in Eq. (31), Eq. (32), and Eq. (33), respectively as follows:

$$\theta_{r1} = sin(0.2\pi t) \quad (31)$$

$$\theta_{r2} = sin(0.2\pi t - \tfrac{\pi}{4}) \quad (32)$$

Received 09/February/2022; Accepted 30/April/2022
 ISSN (Print) 1811-9212 ISSN (Online) 2617-3352

DOI: https://doi.org/10.33103/uot.ijccce.22.4.7

$$\theta_{r3} = sin(0.2\pi t - \frac{\pi}{2}) \quad (33)$$

Where $(\theta_{r1}(0), \theta_{r2}(0), \theta_{r3}(0))$ equal to (0, -0.7, -1) rad and (x (0), y (0)) equal to (1.0769, -0.4580) m. The tuned gains of all proposed controllers are given in Table III and the settling time, rising time, maximum overshoot, and ITSE of the FOFPID & IOFPID controllers are listed in Table IV. *Fig. 8* depicts the performance of all suggested controllers in terms of trajectory tracking curves, controller outputs, and end-effector x–y plots.

TABLE III. THE GAINS OF THE FOFPID & IOFPID CONTROLLERS

Controller	Link NO	K_p	K_d	K_i	K_o	μ	λ
FOFPD-FOPID	L1	K_{p1}=15.7339 K_{p2}=-0.6158	K_{d1}=19.8238 K_{d2}=-13.2834	-7.7518	-	$\mu_1 = 0.3580$ $\mu_2 = 0.3189$	0.9103
	L2	K_{p1}=-31.5902 K_{p2}= 7.9613	K_{d1}= -30.6171 K_{d2}= 5.1884	31.8232	-	$\mu_1 = 0.3758$ $\mu_2 = 0.6228$	0.1313
	L3	K_{p1}=-17.3593 K_{p2}= 34.4328	K_{d1}= -13.2758 K_{d2}= 9.8579	14.3022	-	$\mu_1 = 0.3005$ $\mu_2 = 0.9375$	0.1661
IOFPD-IOPID	L1	K_{p1}= 16.0156 K_{p2}= -17.2883	K_{d1}= -9.3196 K_{d2}=-0.7080	-0.0706	-	-	-
	L2	K_{p1}= 5.5441 K_{p2}= -21.9407	K_{d1}= -4.4321 K_{d2}= -4.5521	-1.7025	-	-	-
	L3	K_{p1}= 20.3293 K_{p2}= -14.8535	K_{d1}= -18.7524 K_{d2}= -8.7990	0.0565	-	-	-
TBFOFPID	L1	K_{p1}= 5.8016 K_{p2}= -25.5027	K_{d1}= -33.8605 K_{d2}= -20.6376	-0.4446	64.7718	0.5094	0.8461
	L2	K_{p1}= -32.0495 K_{p2}= -18.7664	K_{d1}= -37.5642 K_{d2}= -10.686	50.9832	53.5769	0.6691	0.0116
	L3	K_{p1}= 6.8185 K_{p2}= -30.9999	K_{d1}= -8.4111 K_{d2}= -10.3206	-0.8800	18.9430	0.5540	0.3762
TBIOFPID	L1	K_{p1}= 9.6595 K_{p2}= 6.2274	K_{d1}= 72.2229 K_{d2}= 80.5671	11.3271	-69.7011	-	-
	L2	K_{p1}= -10.2655 K_{p2}= -9.2777	K_{d1}= -89.3741 K_{d2}= -85.9593	-2.4651	109.9286	-	-
	L3	K_{p1}= -9.5859 K_{p2}= -8.0307	K_{d1}= -93.6690 K_{d2}= -90.9199	-12.0484	109.4507	-	-
OBFOFPID	L1	-10.3158	-13.8669	-0.7093	51.9787	0.3243	0.9916
	L2	-7.5976	-10.0103	1.0436	47.9278	0.3670	0.9749
	L3	-5.5835	-10.6151	-2.8414	63.9970	0.3688	0.8725
OBIOFPID	L1	5.3597	88.9284	10.5627	-63.3790	-	-
	L2	-8.2201	-90.6135	-3.6173	78.9960	-	-
	L3	-5.9414	-88.1739	-8.3451	60.1748	-	-
FOFPD+I	L1	-9.4215	-5.4440	0.6057	22.5769	0.4798	0.1151
	L2	4.1581	5.1692	8.9371	-21.4793	0.4767	0.6909
	L3	25.9622	12.1831	9.2616	-19.8259	0.3459	0.4058
IOFPD+I	L1	6.5073	57.7893	6.1083	-58.3893	-	-
	L2	4.8261	57.9998	4.3758	-58.9747	-	-
	L3	3.8466	67.9668	-48.9998	-78.8537	-	-

Received 09/February/2022; Accepted 30/April/2022

ISSN (Print) 1811-9212 *ISSN (Online) 2617-3352*

DOI: https://doi.org/10.33103/uot.ijccce.22.4.7

TABLE IV. THE SETTLING TIME, RISING TIME, MAXIMUM OVERSHOOT AND ITSE OF THE FOFPID & IOFPID CONTROLLERS

Controller	Link NO	Settling time	Rising time	Maximum overshoot	ITSE
FOFPD-FOPID	L1	0.0290	0.0370	0.0131	2.7420×10^{-6}
	L2	0.0160	0.0210	0.0106	
	L3	0.0050	0.0070	0.0017	
IOFPD-IOPID	L1	0.1910	0.1030	0.0243	4.1892×10^{-5}
	L2	0.0530	0.0810	0.0095	
	L3	0.0060	0.0090	0.0127	
TBFOFPID	L1	0.0320	0.0280	0.0099	1.6195×10^{-5}
	L2	0.0210	0.0250	0.0198	
	L3	0.1200	0.0590	0.0402	
TBIOFPID	L1	0.5820	0.0740	0.0565	7.0703×10^{-4}
	L2	0.6250	0.0250	0.1334	
	L3	0.5140	0.0540	0.1071	
OBFOFPID	L1	0.1970	0.0290	0.0720	5.5929×10^{-5}
	L2	0.2230	0.0340	0.0707	
	L3	0.1270	0.0300	0.0604	
OBIOFPID	L1	0.6430	0.0730	0.0587	1.2051×10^{-3}
	L2	0.7870	0.0360	0.1244	
	L3	0.8080	0.0770	0.1033	
FOFPD+I	L1	0.2490	0.0490	0.0720	1.7732×10^{-4}
	L2	0.3360	0.0640	0.0542	
	L3	0.3750	0.0480	0.0660	
IOFPD+I	L1	1.4490	0.0640	0.0704	2.1042×10^{-3}
	L2	1.3560	0.0770	0.0717	
	L3	0.6860	0.0870	0.0563	

Received 09/February/2022; Accepted 30/April/2022

 ISSN (Print) 1811-9212 *ISSN (Online) 2617-3352*

DOI: https://doi.org/10.33103/uot.ijccce.22.4.7

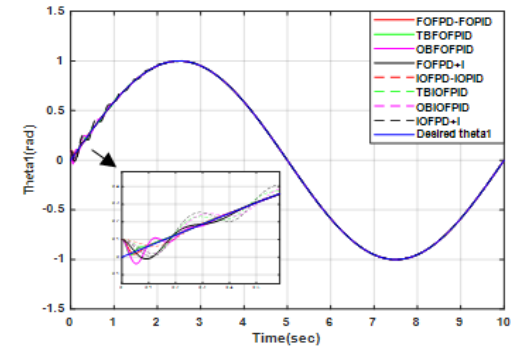

(A)

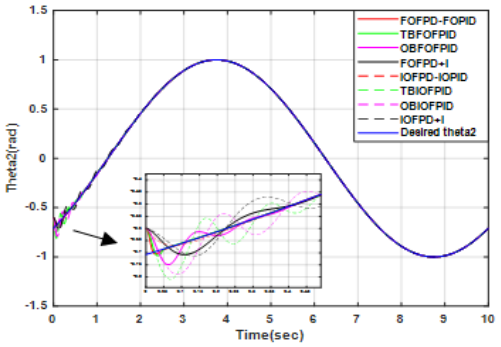

(B)

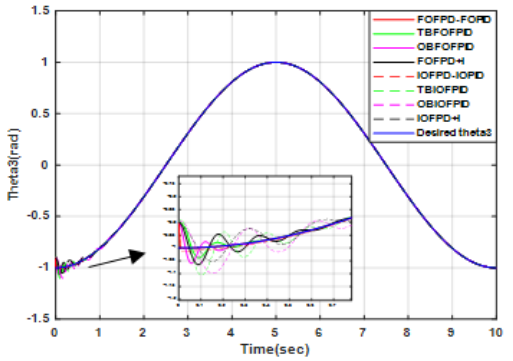

(C)

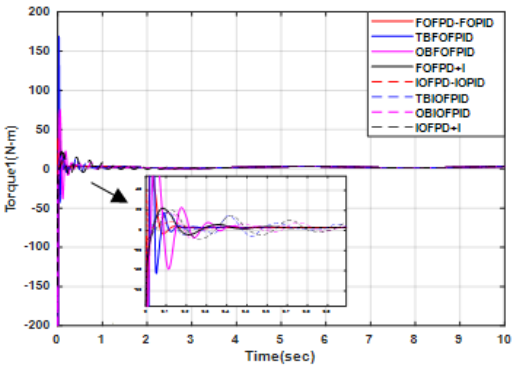

(D)

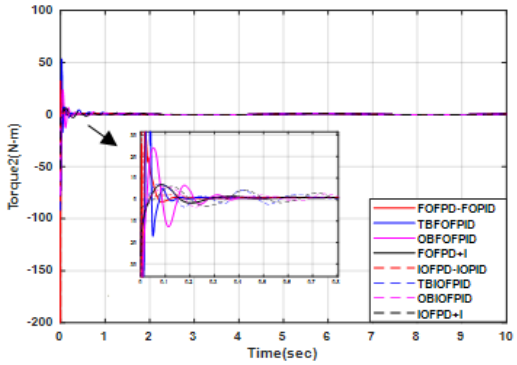

(E)

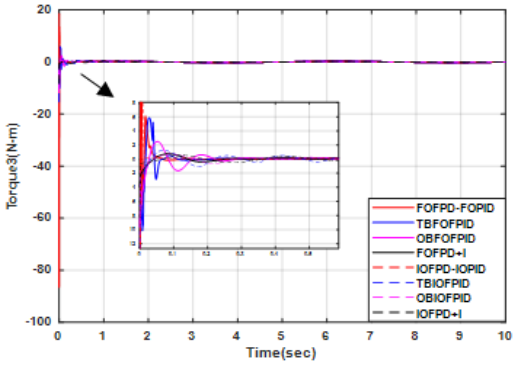

(F)

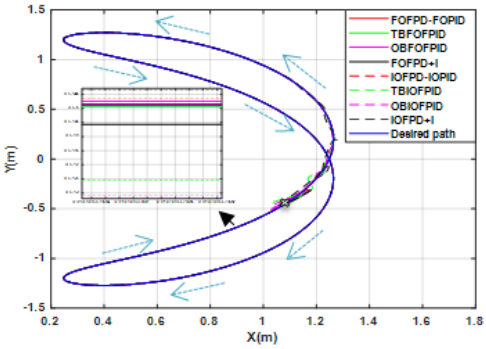

(G)

FIG. 8. (A) DESIRED AND ACTUAL THETA1, (B) DESIRED AND ACTUAL THETA2, (C) DESIRED AND ACTUAL THETA3, (D) CONTROLLER OUTPUT (TORQU1), (E)CONTROLLER OUTPUT (TORQU2), (F)CONTROLLER OUTPUT (TORQU3), AND (G) DESIRED AND ACTUAL PATHS.

Received 09/February/2022; Accepted 30/April/2022

 ISSN (Print) 1811-9212 *ISSN (Online) 2617-3352*

DOI: https://doi.org/10.33103/uot.ijccce.22.4.7

From these results, it can be seen that FOFPID controllers give smoother, faster convergence to the reference trajectory compared with the IOFPID controllers with the least values of ITSE. The FOFPD-FOPID controller is the best controller among all studied controllers since it has the least value of ITSE and the minimum settling time while the IOFPD+I controller is the worst one.

The robustness of FOFPID and IOFPID controllers is investigated by changing the initial positions for theta1, theta2, and theta3 respectively to (0.2,-0.5,-0.8) rad for the trajectory tracking test, and the corresponding ITSE are listed in Table V. The trajectory tracking of theta1, theat2 and theat3 and the path tracked by the end-effector of the 3-LRRM with changing the initial position for all controllers are shown in *Fig. 9*.

TABLE V. THE ITSE OF THE FOFPID & IOFPID CONTROLLERS WITH INITIAL POSITION (0.2,-0.5,-0.8)RAD

controller	ITSE	controller	ITSE
FOFPD-FOPID	1.9848×10^{-4}	IOFPD-IOPID	4.9×10^{-3}
TBFOFPID	1.4×10^{-3}	TBIOFPID	2.2×10^{-3}
OBFOFPID	1.6253×10^{-4}	OBIOFPID	4.1×10^{-3}
FOFPD+I	6.0077×10^{-4}	IOFPD+I	6.9×10^{-3}

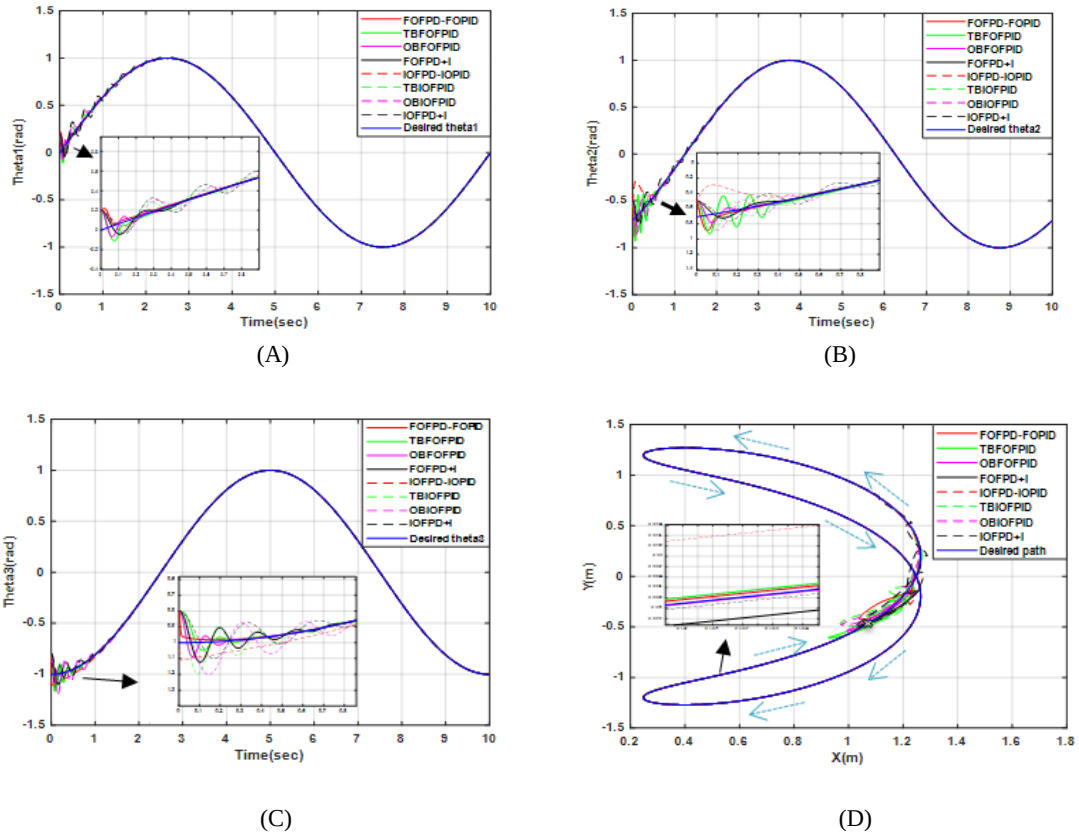

(A) (B)

(C) (D)

FIG. 9. (A) DESIRED AND ACTUAL THETA1, (B) DESIRED AND ACTUAL THETA2, (C) DESIRED AND ACTUAL THETA3, AND (D) DESIRED AND ACTUAL PATHS WITH INITIAL POSITION (0.2,-0.5,-0.8)RAD.

It can be noted that the OBFOFPID controller outperforms all proposed controllers for changing the initial positions of theta1, theta2, and theta3, respectively, where they have the smallest value of ITSE but the FOFPD-FOPID remains has a minimum settling time while the IOFPD+I has a maximum settling time and the largest ITSE.

The disturbance rejection has also been investigated for all proposed controllers by adding the disturbance term [sin (100t)] N-m to the controller output in all three links

Received 09/February/2022; Accepted 30/April/2022

ISSN (Print) 1811-9212 ISSN (Online) 2617-3352

DOI: https://doi.org/10.33103/uot.ijccce.22.4.7

together and making the initial position (0,-0.7,-1) rad without retraining the parameters (gains) of FOFPID and IOFPID controllers as shown in *Fig. 10*. The obtained result is shown in Table VI. The trajectory tracking of theta1, theta2, and theta3, the path tracked by the end-effector of the 3-LRRM using disturbance of [sin (100t)] N-m in all links are presented in *Fig. 11*.

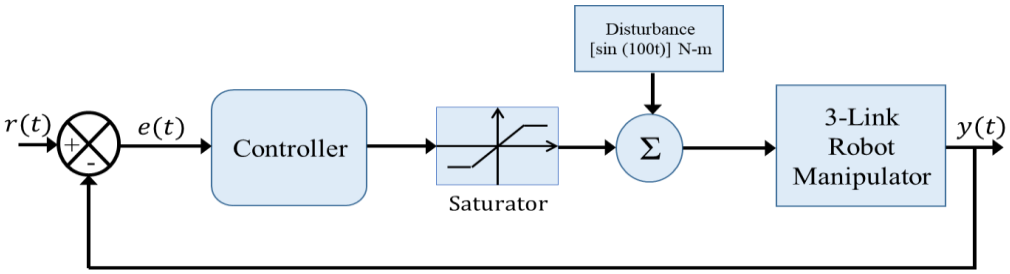

FIG. 10. ADDING DISTURBANCE TO THE CONTROLLER OUTPUT.

TABLE VI. THE ITSE OF THE FOFPID & IOFPID CONTROLLERS WITH DISTURBANCES [SIN (100T)] N-M FOR ALL LINKS

controller	ITSE	controller	ITSE
FOFPD-FOPID	3.4×10^{-3}	IOFPD-IOPID	9.3×10^{-3}
TBFOFPID	3.81×10^{-2}	TBIOFPID	4.12×10^{-2}
OBFOFPID	4.59×10^{-2}	OBIOFPID	7.02×10^{-2}
FOFPD+I	4.4×10^{-2}	IOFPD+I	8.44×10^{-2}

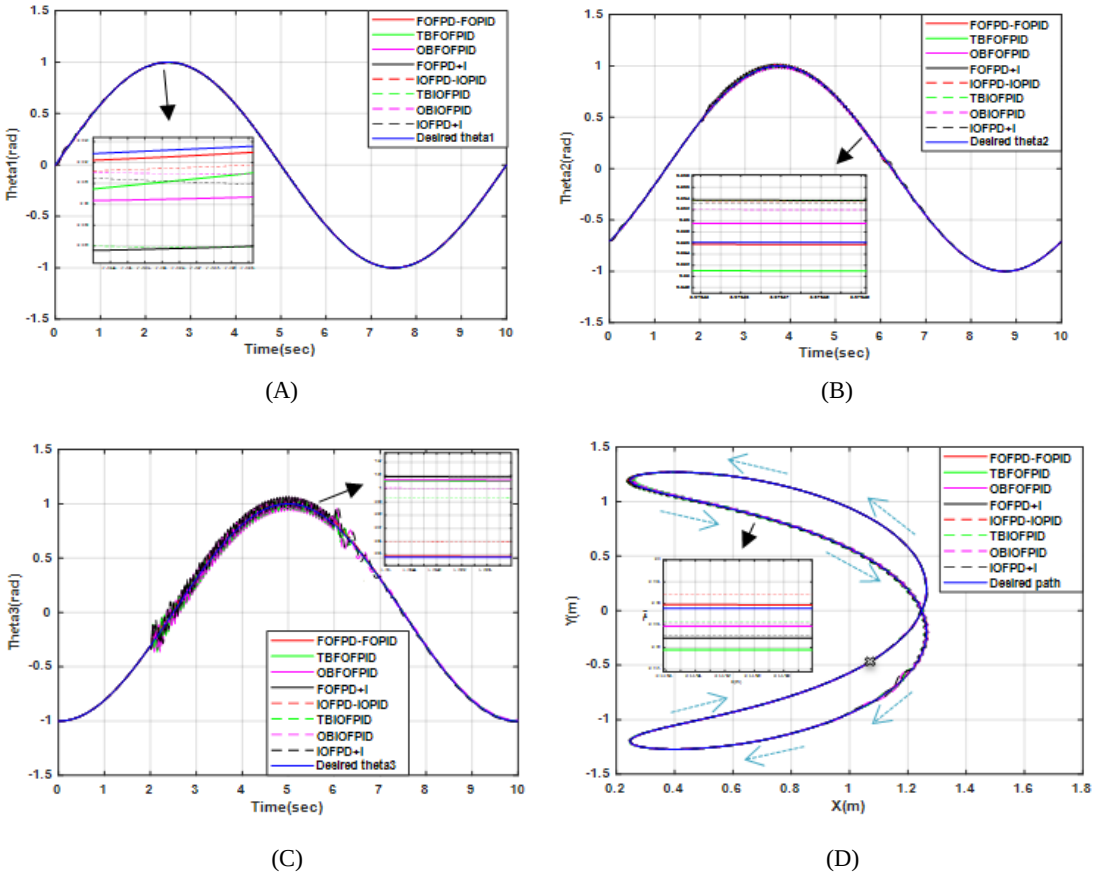

FIG. 11. (A) DESIRED AND ACTUAL THETA1, (B) DESIRED AND ACTUAL THETA2, (C) DESIRED AND ACTUAL THETA3, AND (D) DESIRED AND ACTUAL PATHS WITH DISTURBANCE TERM [SIN (100T)] N-M FOR ALL LINKS AND INITIAL POSITION (0,-0.7,-1)RAD.

Received 09/February/2022; Accepted 30/April/2022

ISSN (Print) 1811-9212 ISSN (Online) 2617-3352

DOI: https://doi.org/10.33103/uot.ijccce.22.4.7

Comparative results clearly show that the suggested FOFPID controllers outperform the other IOFPID controllers for disturbance rejection whereas FOFPD-FOPID is the best one.

The manipulator's major role in the industry is to pick and place objects of various masses using its end-effector so by increasing the masses of link3 by 10% and ensuring the controller parameters remain unaltered, the parameter variation for the FOFPID and IOFPID controllers is also explored. The obtained ITSE is listed in Table VII and the trajectory tracking of theta1, theta2, and theta3 with respect to mass changes for all controllers is presented in *Fig. 12*.

TABLE VII. THE ITSE OF THE FOFPID & IOFPID CONTROLLERS FOR 10% INCREASING IN MASS OF LINK3

controller	**ITSE**	**controller**	**ITSE**
FOFPD-FOPID	2.0108×10^{-4}	IOFPD-IOPID	4×10^{-3}
TBFOFPID	6.5563×10^{-4}	TBIOFPID	1.1×10^{-3}
OBFOFPID	5.8737×10^{-4}	OBIOFPID	2.9×10^{-3}
FOFPD+I	1.6×10^{-3}	IOFPD+I	4.1×10^{-3}

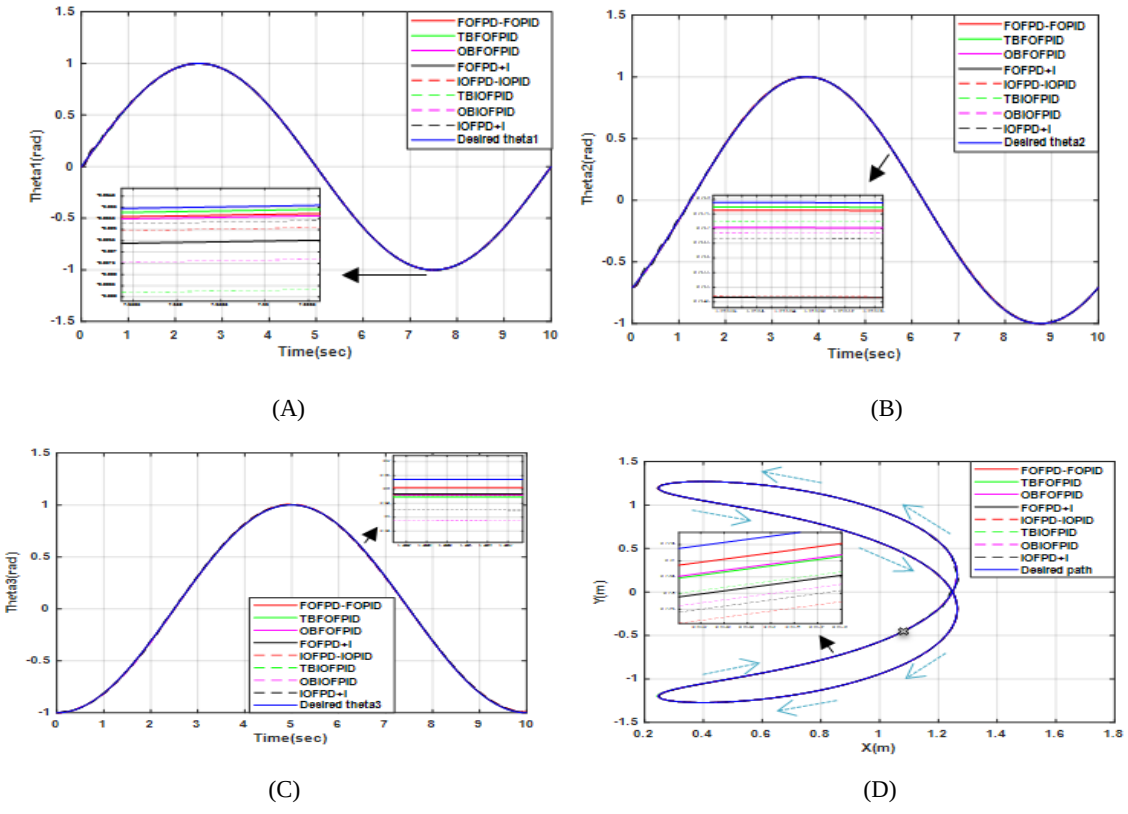

(A) (B)

(C) (D)

FIG. 12. (A) DESIRED AND ACTUAL THETA1, (B) DESIRED AND ACTUAL THETA2, (C) DESIRED AND ACTUAL THETA3, AND (D) DESIRED AND ACTUAL PATHS FOR 10% INCREASING IN MASS OF LINK3 AND INITIAL POSITION (0,-0.7,-1)RAD.

Based on the results, it can be concluded that the ITSE for the FOFPID controllers is less than that of the IOFPID controllers for parameter variation. However, the FOFPD-FOPID is the best among other controllers, the TBFOFPID gives a better response for theta1 and theta2 compared with other controllers. The worst controller is IOFPD+I since it has the largest ITSE .

Received 09/February/2022; Accepted 30/April/2022

ISSN (Print) 1811-9212 *ISSN (Online) 2617-3352*

DOI: https://doi.org/10.33103/uot.ijccce.22.4.7

To show the efficacy of the suggested FOFPID and IOFPID controllers, we combined the effects of adjusting the initial positions, adding disturbance as well as parameter change, The obtained ITSE is listed in Table VIII. *Fig. 13* shows the trajectory tracking of theta1, theta2, and theta3 and the path tracked by the end-effector of the 3-LRRM with respect to changing the initial positions, disturbance as well as parameter variation for all controllers.

TABLE VIII. THE ITSE OF THE FOFPID & IOFPID CONTROLLERS WITH INITIAL POSITION (0.2,-0.5,-0.8)RAD, DISTURBANCES [SIN (100T)] N-M FOR ALL LINKS, AND 10% INCREASING IN MASS OF LINK3

controller	ITSE	controller	ITSE
FOFPD-FOPID	2.4×10^{-3}	IOFPD-IOPID	1.22×10^{-2}
TBFOFPID	3.37×10^{-2}	TBIOFPID	4.01×10^{-2}
OBFOFPID	4.90×10^{-2}	OBIOFPID	6.35×10^{-2}
FOFPD+I	4.37×10^{-2}	IOFPD+I	8.89×10^{-2}

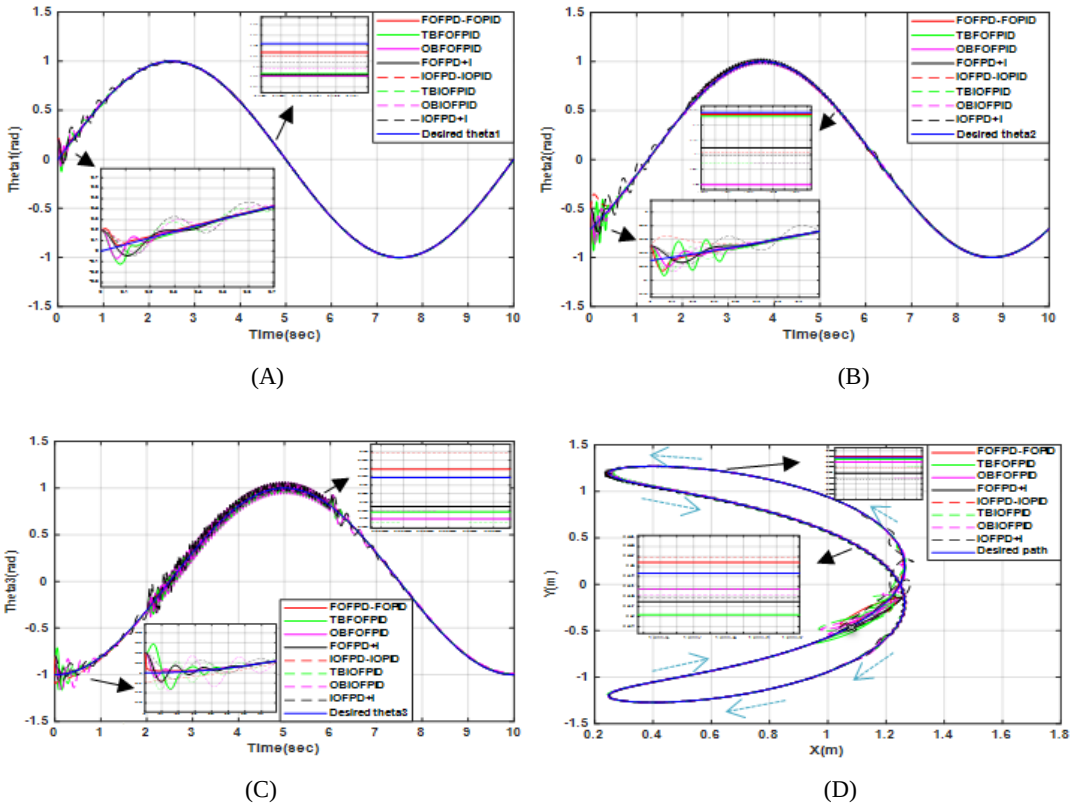

(A) (B)

(C) (D)

FIG. 13. (A) DESIRED AND ACTUAL THETA1, (B) DESIRED AND ACTUAL THETA2, (C) DESIRED AND ACTUAL THETA3, AND (D) DESIRED AND ACTUAL PATHS WITH INITIAL POSITION (0.2,-0.5,-0.8)RAD, DISTURBANCE TERM [SIN (100T)] N-M FOR ALL LINKS AND 10% INCREASING IN MASS OF LINK3.

Even after changing the initial positions, adding disturbance and varying the parameter, the ITSE for the FOFPD-FOPID controller stays the smallest among all proposed controllers. We can see from theta1, theta2, and theta3 responses that it has the minimum settling time whereas the IOFPD+I controller is the worst among all proposed controllers since it has the largest value of ITSE and its response has a maximum settling time.

Received 09/February/2022; Accepted 30/April/2022

ISSN (Print) 1811-9212 *ISSN (Online) 2617-3352*

DOI: https://doi.org/10.33103/uot.ijccce.22.4.7

VI. CONCLUSIONS

A fractional/Integer Order Fuzzy PID controller in four structures is introduced to control the motion of the three-link robotic manipulator at a given trajectory. By minimizing the integral of the time square error, the Most Valuable Player Algorithm is used to optimize the parameters of FOFPID and IOFPID controllers. The controllers' robustness against changing initial conditions, external disturbances, and model uncertainty are thoroughly investigated.

Simulation studies revealed that the FOFPID control system exceeded the IOFPID control scheme in terms of tracking accuracy and control signal chattering with the best controller being the FOFPD-FOPID, followed by the TBFOFPID, the OBFOFPID and finally the FOFPD+I. However, when it came to changing the initial positions, the OBFOFPID with the smallest ITSE was the best controller.

In terms of fast and robust response, the FOFPID controller outperforms the IOFPID controller in all structures with the ITSE for FOFPD-FOPID, TBFOFPID, OBFOFPID, and FOFPD+I for trajectory tracking tasks equal to 2.7420×10^{-6}, 1.6195×10^{-5}, 5.5929×10^{-5} and 1.7732×10^{-4}, respectively whereas the ITSE for IOFPD-IOPID, TBIOFPID, OBIOFPID, and IOFPD+I equal to 4.1892×10^{-5}, 7.0703×10^{-4}, 1.2051×10^{-3} and 2.1042×10^{-3} respectively. The FOFPD-FOPID controller is the best of all the controllers studied.

REFERENCES

[1] Y. J. Huang, "Variable structure control for a two-link robot arm", Electrical Engineering, Vol. 85, No. 4, pp. 195–204, 2003.

[2] V. T. Yen, W. Y. Nan, and P. V. Cuong, "Recurrent fuzzy wavelet neural networks based on robust adaptive sliding mode control for industrial robot manipulators," Neural Computing and Applications, vol. 31, no. 11. pp. 6945–6958, 2018.

[3] S . Fateh & M. M. Fateh, "Adaptive fuzzy control of robot manipulators with asymptotic tracking performance," Journal of Control, Automation and Electrical Systems, vol. 31, no.1.pp. 52-61, 2019.

[4] J. Kumar, V. Kumar, and K. P. S. Rana, "A fractional-order fuzzy PD+I controller for three-link electrically driven rigid robotic manipulator system," Journal of Intelligent and Fuzzy Systems, vol. 35, no. 5. pp. 5287–5299, 2018.

[5] B. Bandyopadhyay and S. Kamal, Stabilization and control of fractional order systems: A sliding mode approach, Springer International Publishing,vol. 317, 2015.

[6] J. Kim, A. S. Lee, K. Chang, B. Schwarz, S. A. Gadsden, and M. Al-Shabi, "Dynamic Modeling and Motion Control of a Three-Link Robotic Manipulator," Proceedings of International Conference on Artificial Life and Robotics, vol. 22. pp. 380–383, 2017.

[7] U. Kabir, M. Hamza, and G. S. Shehu, "Performance Analysis of PID, PD and Fuzzy Controllers for Position Control of 3-Dof Robot Manipulator," Zaria Journal of Electrical Engineering Technology, Department of Electrical Engineering, Ahmadu Bello University, vol. 8, no. 1, 2019.

[8] V. Kumar, K.P.S. Rana, D. Kler, "Efficient control of a 3-link planar rigid manipulator using self-regulated fractional-order fuzzy PID controller," Applied Soft Computing Journal, 82, 105531,2019.

[9] A. M. Abdul-Alsada, K. M. H. Raheem, and M. M. S. Altufaili, "A Fuzzy Logic Controller for a Three Links Robotic Manipulator", AIP Conference Proceedings. Vol. 2386. No. 1. AIP Publishing LLC, 2022.

[10] H. CAO, "Design of a fuzzy fractional order adaptive impedance controller with integer order approximation for stable robotic contact force tracking in uncertain environment", acta mechanica et automatica, Vol. 16, No. 1, 2022.

[11] M. Bhave, L. Dewan, and S. Janardhanan, "A Novel Third Order Sliding Mode Controller for the Orientation and Position of Planar Three Link Rigid Robotic Manipulator," International Conference on Instrumentation Control and Automation,2013.

[12] J. Kumar, V. Kumar, K. P. S. Rana, "Fractional-order self-tuned fuzzy PID controller for three-link robotic manipulator system," Neural Computing and Applications,2019.

[13] S.M. Raafat, and F.A. Raheem, "Introduction to Robotics-Mathematical Issues", Mathematical Advances Towards Sustainable Environmental Systems . Springer, Cham, pp. 261-289, 2017.

[14] F. L. Lewis, D. M. Dawson, and C. T. Abdallah, Robot Manipulator Control Theory and Practice, CRC Press, pp. 1–632, 2004.

[15] S. Kucuk and Z. Bingul, "Robot Kinematics: Forward and Inverse Kinematics," Industrial Robotics: Theory, Modelling, and Control. 2006.

[16] F. Piltan, M. Yarmahmoudi, M. Mirzaie, S. Emamzadeh, and Z. Hivand, "Design Novel Fuzzy Robust Feedback Linearization Control with Application to Robot Manipulator," I.J. Intelligent Systems and Applications, vol. 5, no.

Received 09/February/2022; Accepted 30/April/2022
 ISSN (Print) 1811-9212 *ISSN (Online) 2617-3352*

DOI: https://doi.org/10.33103/uot.ijccce.22.4.7

5, pp. 1–10, 2013, DOI: 10.5815/ijisa.2013.05.01.

[17] F. A. Raheem, B. F. Midhat, and H. S. Mohammed, "PID and Fuzzy Logic Controller Design for Balancing Robot Stabilization," Iraqi J. Comput. Commun. Control Syst. Eng., vol. 18, no. 1, pp. 1–10, 2018.

[18] A. Mehiri, R. Fareh, "Comparison study on advanced control of Two 2DOF Manipulator robots," International Conference on Electrical and Computing Technologies and Applications.IEEE.pp.1-5,2017.

[19] H. Delavari, R. Ghaderi, N. Ranjbar, S. H. Hosseinnia, and S. Momani, "Adaptive Fractional PID Controller for Robot Manipulator," Proc. 4th IFAC Work. Fract. Differ. Its Appl., vol. 2010, pp. 1–7, 2010.

[20] H. M. Kadhim, and A. A. Oglah , "Interval type-2 and type-1 Fuzzy Logic Controllers for congestion avoidance in internet routers", In: Proc. of International Conf. On Sustainable Engineering Techniques, Vol. 881, No. 1, p. 012135, 2020.

[21] D. M. Wonohadidjojo, G. Kothapalli, and M. Y. Hassan, "Position Control of Electro-hydraulic Actuator System Using Fuzzy Logic Controller Optimized by Particle Swarm Optimization", International Journal of Automation and Computing, Vol. 10, No. 3, pp. 181-193, 2013.

[22] W. I. M. AL-Tameemi, W. M. H. Hadi, "Modeling and Control of 5250 Lab-Volt 5 DoF Robot Manipulator," vol. 15, no. 2, pp. 34–46, 2015.

[23] K. M. Passino, S. Yurkovich, Fuzzy Control, 1998.

[24] J. R. B. A. Monteiro, W. C. A. Pereira, M. P. Santana, T. E. P. Almeida, G. T. Paula, and I. Santini, "Anti-windup method for fuzzy PD+ I, PI and PID controllers applied in brushless DC motor speed control," Brazilian Power Electronics Conference.IEEE, pp. 865-871,2013.

[25] A. Vasičkaninová, M. Bakošová, J. Oravec, and M. Horváthová, "Efficient fuzzy control of a biochemical reactor," Chemical Engineering Transactions, vol. 81. pp. 85–90, 2020.

[26] E. Yesil, M. Guzelkaya & I. Eksin, " Fuzzy PID controllers: An overview," The Third Triennial ETAI International Conference on Applied Automatic Systems, Skopje, Macedonia, pp. 105-112,2003.

[27] M. J. Mohamed and M. Y. Abbas, "Design Interval Type-2 Fuzzy Like (PID) Controller for Trajectory Tracking of Mobile Robot", Iraqi Journal of Computers, Communications, Control and Systems Engineering , Vol. 19, No. 3, pp. 1–15, 2019.

[28] P. C. Pradhan, R. K. Sahu, and S. Panda, "Firefly algorithm optimized fuzzy PID controller for AGC of multi-area multi-source power systems with UPFC and SMES," Engineering Science and Technology, an International Journal, vol. 19, no. 1. pp. 338–354, 2015.

[29] H. Khattab, A. Sharieh, and B. A. Mahafzah, "Most valuable player algorithm for solving minimum vertex cover problem," Int. J. Adv. Comput. Sci. Appl., vol. 10, no. 8, pp. 159–167, 2019.

[30] H. R. E. H. Bouchekara, "Most Valuable Player Algorithm: a novel optimization algorithm inspired from sport," Springer Berlin Heidelberg, vol. 20, no. 1, 2017.

Received 09/February/2022; Accepted 30/April/2022

 ISSN (Print) 1811-9212 *ISSN (Online) 2617-3352*